CHARACTERIZATION OF POLY L-LACTIDE/HYDROXYAPATITE COMPOSITE: CHEMICAL, THERMAL AND THERMOMECHANICAL PROPERTIES

CARMEN ALBANO[1], GEMA GONZÁLEZ[2], JORDANA PALACIOS[3], ARQUÍMEDES KARAM[3], REINA VERÓNICA CASTILLO[3], MARÍA COVIS[3]

[1]Universidad Central de Venezuela, Facultad de Ingeniería, Caracas, Venezuela.

*e-mail: carmen.albano@ucv.ve

[2]Instituto Venezolano de Investigaciones Científicas, Departamento de Ingeniería de Materiales y Nanotecnología, Caracas, Venezuela.

[3]Instituto Venezolano de Investigaciones Científicas, Centro de Química, Laboratorio de Polímeros, Caracas, Venezuela.

Recibido: julio 2012 Recibido en forma final revisado: enero 2013

ABSTRACT

The chemical, thermal, thermo-mechanical and morphology properties of poly (L-lactide) (PLLA) composite with 30% hydroxyapatite (HA) were evaluated. The composite was prepared employing the solvent casting technique. Hydroxyapatite was synthesized by chemical precipitation method. The degradation kinetic parameters were calculated using the Coats – Redfern integral method to obtain the reaction order and the E_2 function methodology to calculate the activation energy (*Ea*). The addition of HA to PLLA matrix increased its glass transition temperature. This was confirmed by DSC and DMTA analysis. Also, the presence of HA increased the crystallization temperature of PLLA, implying a nucleation effect. The PLLA-HA composite exhibited better thermal stability than the neat polymer; additionally higher decomposition temperature and activation energy for the decomposition process were obtained. HA nanoparticles have a rod shape morphology that might improve the interfacial interactions, increasing the thermal stability of the composite. The storage modulus (E') of this composite was enhanced mainly at temperatures above the glass transition.

Keywords: PLLA composites, Hydroxyapatite, Thermal degradation, DMTA.

CARACTERIZACIÓN DEL COMPUESTO POLI (L-LACTIDA) / HIDROXIAPATITA: PROPIEDADES QUÍMICAS, TÉRMICAS Y TERMOMECÁNICAS.

RESUMEN

Estudios químicos, térmicos, termomecánicos y morfológicos se realizaron al PLLA solo y al compuesto de polylactida-L (PLLA) con 30% en peso de hidroxiapatita (HA). Los compuestos fueron preparados por la técnica de solución. La hidroxiapatita fue sintetizada por el método de precipitación química. Los parámetros cinéticos como el orden de reacción y la energía de activación se obtuvieron utilizando los métodos integrales de Coats – Redfern y Función E_2, respectivamente. La temperatura de transición vítrea del PLLA se incrementó con la adición de HA, estos resultados fueron confirmados por los estudios realizados por DSC y DMTA. También, la temperatura de cristalización del PLLA se incrementó con la presencia de HA en el compuesto, lo que implica un efecto nucleante. Adicionalmente, la temperatura de descomposición y la energía de activación son mayores en el compuesto (PLLA-HA) que en el polímero solo, lo que implica que el compuesto muestra una mayor estabilidad térmica. La morfología tipo aguja de la HA pudo haber mejorado las interacciones interfaciales, y por tanto, la estabilidad térmica del compuesto. Por último, el modulo de almacenamiento (E´) de este compuesto se mejoró a temperaturas por encima de la temperatura de transición vítrea.

Palabras clave: Compuestos de PLLA, Hidroxiapatita, Degradación térmica, DMTA.

INTRODUCTION

The addition of specific nanoparticles to a polymeric matrix enhances the properties and broadens the field of application of polymers. For these reasons, over the past few decades, researchers have been focused on the development of better and improved polymer composites evaluating different nanofillers like organoclays (Pavlidoua & Papaspyridesb, 2008; Bordes *et al.* 2009), carbon nanotubes (CNT) (Sahoo *et al.* 2010; Spitalsky *et al.* 2010) and hydroxyapatite (HA) (Rezwan *et al.* 2006; Roeder *et al.* 2008).

Hydroxyapatite has been intensively investigated as bone repair material due to its chemical composition ($Ca_{10}(PO_4)_6(OH)_2$) (Rezwan *et al.* 2006) and structure, which is similar to the main inorganic constituent of natural bone, and also to their bioactive, biocompatible, and osteoconductive properties (Kokubo *et al.* 2003; Kumta *et al.* 2005; Rezwan *et al.* 2006; Zhou *et al.* 2007; Roeder *et al.* 2008). However, their low mechanical fracture performance and high brittleness restrict their application in bone regeneration at high load-bearing sites (Kokubo *et al.* 2003).

The combination of HA properties with those of the polymeric matrices seem to be promising for bone tissue engineering purposes, due to a good combination of flexural strength and high toughness [8]. To accomplish this improvement, HA particles should exhibit an acicular structure with nanometric size (Kokubo *et al.* 2003; Kothapalli *et al.* 2005; Li & Wang, 2005; Zhou *et al.* 2007); this morphology promotes a better interaction and load transfer between the filler and the matrix.

Different biodegradable polymers (Nair & Laurencin, 2007) have been used as biomaterials for bone tissue engineering applications, some poly(α-esters)/HA composites have attracted much interest due to their good biocompatibility, specific biodegradability and good mechanical properties. Among them, the most employed composites with HA are Poly(lactide) (PLA) and its stereoisomeric forms, poly(glycolide) (PGA) and poly(lactide-co-glycolide) (PLGA) copolymer (Shikinami & Okuno,. 1999; Kim *et al.* 2006; Petricca *et al.* 2006; Lee *et al.* 2008; Cui *et al.* 2009; Chłopek *et al.* 2009; Aboudzadeh *et al.* 2010; Zhang *et al.* 2010). These polymers are FDA approved and therefore exhibit biocompatible properties. In addition, they are easily processed and their physical and mechanical properties and degradation features can be adjusted by copolymerization (Shikinami & Okuno, 1999; Kim *et al.* 2006; Petricca *et al.* 2006; Lee *et al.* 2008; Cui *et al.* 2009; Chłopek *et al.* 2009; Aboudzadeh *et al.* 2010; Zhang *et al.* 2010).

PLA-HA composites have been synthesized through several methods, focusing in most of the cases on the final application. Solution mixing and in-situ precipitation were employed in order to characterize and evaluate the properties of the composite material. Zhang *et al.* (2010) used a modified in situ precipitation method to prepare PLLA/nano-HA composites, obtaining a well distributed HA and improvement on Young's modulus and compressive strength. Scaffolds based on PLA-HA composites have been obtained using many different methods: thermally induced phase separation (Nejati *et al.* 2008), porogen-leaching (Li *et al.* 2010), rapid prototyping technique (Li *et al.* 2010), electrospinning (Peng *et al.* 2011), and electrospun techniques (Seyedjafari *et al.* 2010). In general, these works deal with the bioactive performance of the composite device for a bone tissue engineering application and less emphasis is made on the physico- chemical, thermal and mechanical properties of the composite.

In the present work PLLA with 30 wt. % HA composite was prepared to elucidate the effect of HA on the chemical, mechanical, thermal and thermal degradation properties of PLLA. The filler content (30wt. % HA) was chosen based on previous studies conducted (Albano *et al.* 2009; Albano *et al.* 2010; Albano *et al.* 2010). The kinetics of the thermal degradation of the composites using the Coats – Redfern integral method (Coats & Redfern, 1964) was evaluated to obtain the reaction order, and the E2 function method (Chen *et al.* 2004) was used to calculate the activation energy.

EXPERIMENTAL

Materials

A Poly(L-lactide) (PLLA) homopolymer from Sigm-Aldrich, was used as polymer matrix (Lactel® BP-0600, Mw: 66.000-107.000). For the HA synthesis, calcium hydroxide ($Ca(OH)_2$) 98,6% and ammonium hydrogen phosphate ($(NH_4)_2HPO_4$) 99%, (Fisher Chemicals), were used as starting materials. Chloroform 99.8% supplied by Merck was employed as the solvent for composite preparation.

Synthesis of hydroxyapatite

The synthesis of HA was carried out according to ref (Spadavecchia & González, 2007). Stoichiometric deionized water solutions of $Ca(OH)_2$ and $(NH_4)_2HPO_4$ were prepared by magnetic stirring for 30min. Then, $(NH_4)_2HPO_4$ solution was transferred to an addition funnel and dropped into $Ca(OH)_2$ solution under continuous stirring. After that, the reaction was allowed to continue for 30min. Then, the mixture was decanted for 3 days. The solid obtained was centrifuged and washed with de-ionized water repeatedly until neutral pH was achieved. The HA was vacuum-dried at 60ºC for 62h. Finally, it was grinded and sieved until a fine powder was obtained.

Composite preparation

The composite (PLLA-HA) was prepared by solvent casting technique using chloroform as solvent. Specific quantities of PLLA and HA were separately dissolved and suspended,

respectively, in chloroform for 4 hours. After that, the PLLA solution was slowly added to the HA suspension under continuous magnetic stirring for 4 hours. Then, the mixture was poured into a petri dish and allowed to dry at room temperature to remove the excess of solvent and later in a vacuum oven for a week.

Characterization

Crystallographic analysis of the synthesized HA was performed in a SIMENS D5005 diffractometer. The XRD data were recorded using Cu*K*α radiation (λ = 0.15406nm) and the diffraction patterns were scanned between 10 and 80º (2θ) with step size of 0.02º and 0.52s counting time per step.

Fourier infrared spectroscopy was carried out for the pure components and composite in a Thermo Scientific Nicolet iS10 spectrometer with a resolution of 4cm^{-1}. HA powdered sample was prepared with KBr and the spectrum was recorded in transmission mode between 4000 and 400cm^{-1} (32 scans). The composite film was evaluated by Attenuated Total Reflection (ATR) technique between 4000 and 650 cm-1 (32 scans, 4cm^{-1} resolution).

In order to evaluate the thermal properties of the samples, 10 mg of material were encapsulated in aluminum pan and tested in a Mettler–Toledo DSC 822 differential scanning calorimeter under nitrogen atmosphere. The equipment was calibrated with indium standard. The dynamic thermal program employed was as follows: a first heating from 25°C to 70°C at 30°C/min to erase the thermal history, following by a cooling down to 0°C, and a second heating up to 70°C, at 10°C/min.

The thermal stability was studied by thermogravimetric analysis (sample mass 10mg), employing a Mettler–Toledo TGA/SDTA 851 thermal analyzer under nitrogen atmosphere. The equipment was calibrated with indium and aluminum standards. The non-isothermal tests were carried out from 25 to 700ºC at 10°C/min. The thermograms obtained were analyzed employing the Coats-Redfern kinetic models (Coats & Redfern, 1964) and the E_2 function method (Chen *et al.* 2004) to determine the global activation energy value (Ea).

Equation (1) was used to determine the reaction order *n* according to Coats-Redfern method:

$$\ln\left(\frac{G(\alpha)}{T^2}\right) = \ln\left(\frac{AR}{Ea\beta}\right) - \frac{Ea}{2.3RT} \qquad (1)$$

Using the previous expression and the G(α) functions (Mamleev *et al.* 2000; Bourbigot *et al.* 2001; Budrugeac *et al.* 2001), the reaction order *n* was determinate from the best fit of equation (1) suggesting the reaction mechanism.

With *n* known, the E_2 function method (Chen *et al.* 2004) was used to determine Ea and A values, using equations (2) and (3):

$$\frac{\ln\left[\frac{(1-\alpha_1)}{(1-\alpha_2)}\right]}{\ln\left[\frac{(1-\alpha_2)}{(1-\alpha_3)}\right]} = \frac{T_2 \cdot E_2\left(\frac{E_a}{R \cdot T_2}\right) - T_1 \cdot E_2\left(\frac{E_a}{R \cdot T_1}\right)}{T_3 \cdot E_2\left(\frac{E_a}{R \cdot T_3}\right) - T_2 \cdot E_2\left(\frac{E_a}{R \cdot T_2}\right)} \qquad (2)$$

$$\ln\left[\frac{(1-\alpha_1)}{(1-\alpha_2)}\right] = \frac{A}{\beta}\left[T_2 \cdot E_2\left(\frac{E_a}{R \cdot T_2}\right) - T_1 \cdot E_2\left(\frac{E_a}{R \cdot T_1}\right)\right] \qquad (3)$$

The activation Energy Ea is calculated using three conversion values (α_1, α_2 and α_3) and three corresponding decomposition temperatures (T_1, T_2 and T_3).

The mechanical properties were evaluated by dynamic – mechanical – thermal analysis (DMTA) using a Rheometrics Solids Analyzer RSA II in tension mode, film geometry. Rectangular film samples (22 mm long, 8 mm width, 0.1 mm thickness) were employed. A dynamic temperature ramp was recorded from 25 to 100ºC at 1ºC/min, with a frequency of 1 Hz and 0.015% strain. This strain value was previously determined using a dynamic strain sweep test at 1Hz, using the value located in the linear viscoelastic zone. The storage modulus (E') and the loss factor (tan δ) of PLLA and the composite were measured.

The morphology and dispersion of HA in the polymer matrix were evaluated by transmission electron microscopy (TEM) using a JEOL JEM 1220. The samples were prepared by ultramicrotomy method using a RMC PT-X ultramicrotome.

RESULTS AND DISCUSSION

Characterization of the synthesized HA

The FT-IR spectrum of the synthesized HA is presented in Figure 1. The small signal around 3567 cm^{-1} belongs to the stretching mode of the hydroxyl group (OH) present in HA. A broad absorption band located at 3423 cm^{-1} and a band at 1638 cm^{-1} associated to the bending (ν2) mode, corresponding to adsorbed water are present. The four vibrational modes of the phosphate ions of HA are located at 470 cm^{-1} for the double degenerated bending (ν2) mode of the O–P–O bonds; at 565 and 603 cm^{-1} for the triply degenerated bending (ν4) mode of the O–P–O bonds (well-

defined bands); at 962cm^{-1} (very weak signal) for the non-degenerated symmetric stretching (ν1) mode of the P−O bond; and at 1033 and 1096 for the triply degenerated asymmetric stretching (ν3) mode of the P−O bond of the phosphate group (Zhou *et al.* 2007). Also, the vibration bands located between 1500 and 1400 cm^{-1} and at 875cm^{-1} are indicative of the carbonate groups. These groups show three vibrational modes: the bending modes (ν3 or ν4) signals situated at 1453 and 875 cm^{-1}, and the stretching mode (ν3) located at 1413cm^{-1} (Zhou *et al.* 2007). These signals are characteristic of the presence of carbonates in substitution of some of the hydroxyl groups, consequence of the interaction between HA and ambient CO_2 during the synthesis (Wang *et al.* 2007).

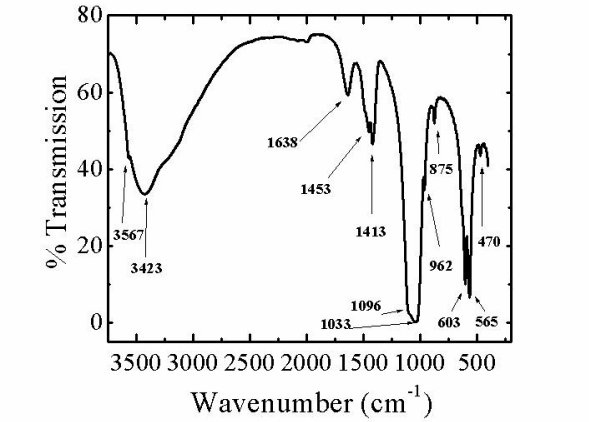

Figure 1. *FT-IR spectra of the synthesized HA*

The crystallographic structure of the HA was also confirmed by x-ray diffraction analysis (Figure 2), and the needle shape morphology of average dimensions of 74 ± 21 nm long and 22 ± 7 nm width, was observed by TEM (Figure 3). The high aspect ratio of HA nanocrystals results in a high interfacial area, this is an important feature to improve the contact area between these nanoparticles and the matrix in polymer composites, improving the mechanical reinforcement.

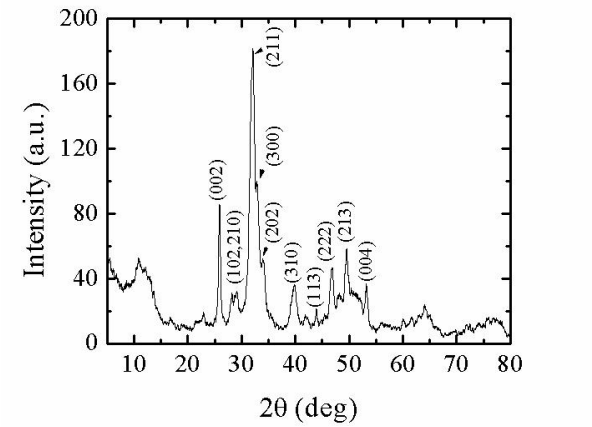

Figure 2. *XRD pattern of synthesized HA*

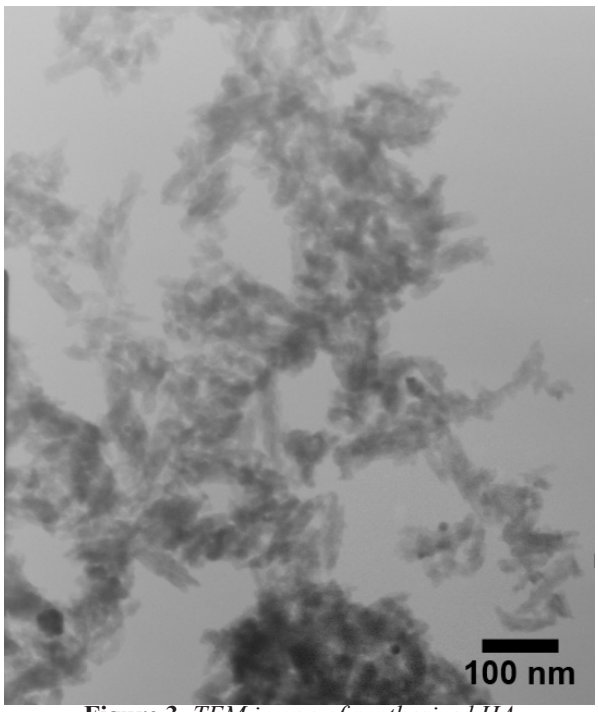

Figure 3. *TEM image of synthesized HA*

The thermal analysis of HA is shown in Figure 4. The total mass loss of this nanoceramic is 11%. Three differentiated regions can be observed, the first region from 25 to 250°C, is associated to the loss of the physically adsorbed water molecules. The second stage between 250-550 °C could be attributed to the slow loss of carbonate ions on the HA , the last region is associated to the slow dehydroxylation of HA (Ivanova *et al.* 2001).

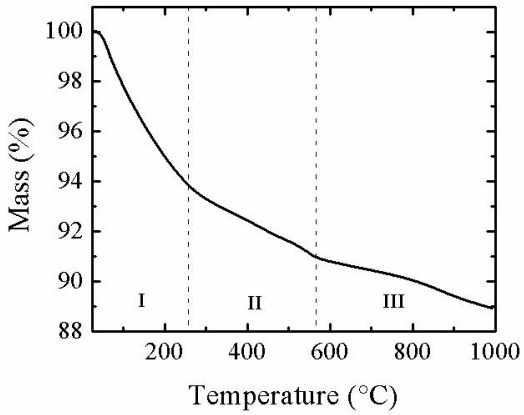

Figure 4. *Non-Isothermal TGA curve of the synthesized HA*

Chemical characterization of the PLLA-HA composite by FTIR

The FT-IR spectra of Poly (L-lactide), PLLA-HA and HA is shown in Figure 5. The spectrum of PLLA presents a signal located at 1748 cm-1 associated to the stretching

mode of the carbonyl group and the vibrations at 1180 and 1080 cm^{-1} corresponding to the symmetric and asymmetric C-O-C stretching modes of the ester groups. The spectrum of PLLA-HA composite shows a shift in the position of the band associated to the phosphate group of HA, from 1033 cm-1 to 1020 cm^{-1}, overlapping the νC-CH_3 stretching of PLLA (Table 1). Also, the band at 1638 cm^{-1}, associated to the bending (ν2) mode of adsorbed water molecules, is shifted to 1605 cm-1 in the composite. A slightly displacement of the carbonyl signal from 1748 cm^{-1} to 1755 cm^{-1} is also observed in the composite spectrum. This band splits in two peaks (inset Figure 5), attributed to interaction of the hydrogen bond of the carbonyl group of PLLA and HA (Zhou *et al.* 2007). Therefore, the different displacements observed suggest possible interactions between the functional groups of the HA and the polymer matrix.

Table 1. Vibrational assignments of PLLA, HA and PLLA-HA composite

Wavenumbers (cm^{-1})	PLLA Vibrational assignments	Wavenumbers (cm^{-1})	HA Vibrational assignments	PLLA-HA Displaced Wavenumbers (cm^{-1})
		3567	OH Stretching	
		3423	ν2H_2O (absorbed) bending	
2995	$\nu_{as}CH_3$ Asymmetric stretching			
2946	$\nu_{s}CH_3$ Symmetric stretching			
2879	νCH Stretching			
1748	νC=O Stretching			1755
		1638	ν2H_2O (absorbed)	
bending	1605			
		1453	ν3,ν4CO_3 bending	
1452	$\delta_{as}CH_3$ Asymmetric bending			
		1413	ν3CO_3 stretching	
1382-1358	$\delta_{s}CH_3$ Symmetric bending			
1180	ν_{s}C-O-C Symmetric stretching			
1127	$r_{as}CH_3$ Asymmetric rocking			
		1096	ν3P−O triply degenerated	
asymmetric stretching				
1080	ν_{as}C-O-C Asymmetric stretching			
1043	νC-CH_3 Stretching			
		1033	ν3P−O triply degenerated asymmetric stretching	1020
		962 (weak)	ν1P−O non-degenerated symmetric stretching	
		875	ν3,ν4CO_3 bending	
868	νC-COO Stretching			
753	δC=O Bending			
		565, 603	ν4O−P−O triply degenerated bending	
		470	ν2O−P−O degenerated bending	

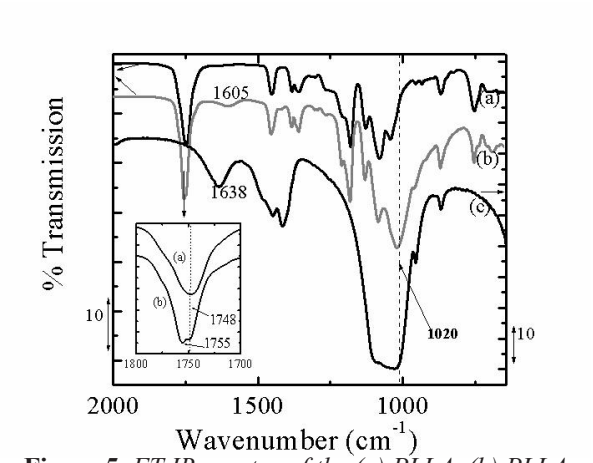

Figure 5. *FT-IR spectra of the (a) PLLA, (b) PLLA composite with HA and (c) HA*

Morphology of PLLA-HA composite

The distribution of HA on the polymer matrix was analyzed by TEM (Figure 6). It can be observed that the nanoparticles are well distributed in the polymer matrix, preserving the rod shape morphology; although some agglomeration was obtained. It is possible that the solvent casting methodology employed to prepare the PLLA-HA composites is not entirely effective to promote a high dispersion of the filler, this could be due to the high content of HA. Similar results have been reported previously in HDPE-HA composites obtained by solution method (Albano *et al.* 2006).

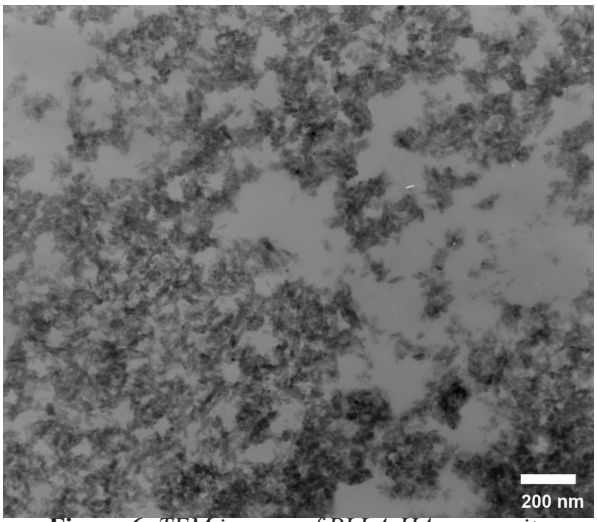

Figure 6. *TEM images of PLLA-HA composite*

Thermal behavior study by DSC of the PLLA-HA composite

The thermograms of PLLA and PLLA-HA are shown in Figure 7 and the results are presented in Table 2. For PLLA, the exothermal peak at 94.5 ºC corresponds to the crystallization temperature (T_{mc}) (see Fig. 7 (a)). During the heating scan, PLLA presents its glass transition temperature (T_g) at 52.5ºC, and a cold crystallization exothermal peak (T_{cc}) at 102.9 ºC and an endothermal peak (T_m) at 172.2 ºC corresponding to the melting transition (see 7 (b)), these values are within the range reported in the literature (Velde & Kiekens,. 2002; Nair *et al.* 2007; Wilberforce *et al.* 2011). The presence of a cold crystallization process is a consequence of the slow crystallization kinetics of PLLA during cooling.

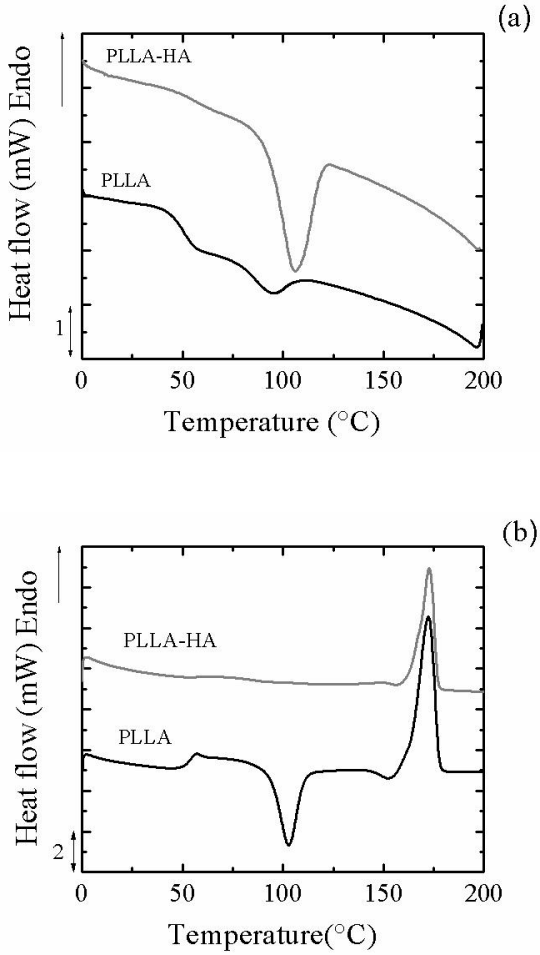

Figure 7. *Non-Isothermal DSC scans of neat PLLA and PLLA-HA composite: (a) Cooling scans at 10ºC/min, (b) Subsequent heating scans at 10ºC/min after the previous cooling run*

The lowest crystallization enthalpy value (-4.99J/g; Table 2), suggests the formation of less perfect and stable crystallites. These would act as self-nuclei for the cold crystallization during heating, along with a spontaneous nucleation from the remaining amorphous phase (Wang & Mano, 2005).

Table 2. DSC Thermal transitions for the PLLA composite with HA

Sample	T_g (°C)	T_{cc} (°C)	T_{mc} (°C)	T_r (°C)	T_m (°C)	ΔH_{cc} (J/g)	ΔH_{mc} (J/g)	ΔH_r (J/g)	ΔH_m (J/g)	$\%X_c$
PLLA	52.5	102.9	94.5	152.3	172.2	-29.66	-4.99	-2.08	41.85	45
PLLA-HA	58.1	-	105.9	156.5	172.7	-	-33.44	-0.63	37.96	41

Besides the cold crystallization and the melting transition, an exothermal peak located just before the melting temperature of PLLA at 152. 3 ºC was observed (identified as Tr in Table 2). This behavior could be explained by the melt-recrystallization model (Yasuniwa *et al.* 2004; Aboudzadeh *et al.* 2010), which suggests that smaller and less perfect crystallites would change into more stable forms, as the temperature increases. So the melting and recrystallization process are competitive during heating and this exothermic peak would appear when the rate of recrystallization overcomes that of the melting process (Yasuniwa *et al.* 2004).

Once HA is incorporated into PLLA matrix, it is clear that these nanoparticles would act as nucleating agents [35] and promote the crystallization of the polymer matrix during cooling. This is evident by the narrow peak observed in PLLA-HA composite thermogram (Figure 7(a)). Additionally, the presence of HA suppresses the cold crystallization and melt-recrystallization process observed in neat PLLA. Deplaine *et al.* (2010) reported a decrease in the cold crystallization temperature in PLLA-HA membranes, with a filler content up to 15 %wt. HA. In our case, the high HA content could induce the nuclei and crystal growth during the cooling, so more stable crystals are formed and no reorder or additional recrystallization occurs during heating.

The composite PLLA-HA showed an increase of 6 ºC on the transition temperature, respect to PLLA (Table 2). The HA nanoparticles reduce the chain segment mobility of the polymeric amorphous phase around them, so the glass transition will occur at higher temperatures (Pham *et al.* 2003; Grady *et al.* 2009). Also, the increase on Tg has been attributed to the existence of some interfacial interactions or non-covalent bonding between HA and the polymer matrix, that restricts the movements of the polymer chains, consistent with FT-IR analysis. An increase in the crystallization temperature of 10 ºC was observed, while no major changes on its melting temperature and crystallinity degree were present. The increase on the crystallization temperature indicates a nucleation effect of the HA nanoparticles, with no detriment on the crystallinity of the polymer matrix. This behavior has been previously observed with different fillers into polymer matrices (Reyes-de-Vaaben *et al.* 2008).

Thermal degradation behavior of the PLLA composite

Figure 8(a) shows the thermograms obtained by TGA for PLLA, PLLA-HA and HA. The PLLA thermogram shows a single step around 360 °C, however, also a shoulder around 340ºC is observed in the derivative graph (Figure 8(b)). It is known that these polyesters exhibit a degradation mechanism that could involve a random chain scission at the beginning of the decomposition and specific chain scission at the end. At lower temperatures, the main degradation mechanism for neat poly(lactide) involves a non-radical, backbiting ester interchange reaction involving OH chain ends, leading mostly to cyclic oligomers rather than linear, or acetaldehyde plus carbon dioxide. As the temperature increases the release of carbon monoxide, methylketene and ketene, as main degradation products are produced as a consequence of a radical chain scission mechanism (McNeill & Leiper, 1985).

The addition of 30% HA to PLLA matrix improves the thermal stability of the polymer, as can be seen in Figure 8. A rise on the initial decomposition temperature (Tonset) and on the degradation peak temperature (Tpeak) was observed for PLLA, in the composite (Table 3). On the other hand, an increase on the degradation rate of the polymer matrix was observed with the presence of the HA (Figure 8 (b)). Also, an increase in the activation energy of the polymer in PLLA-HA composite was obtained. Therefore, HA improves the thermal stability of PLLA, but once the degradation process is initiated, the decomposition rate is high.

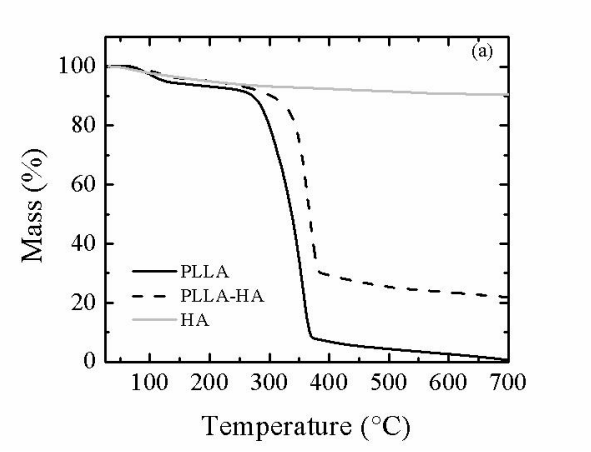

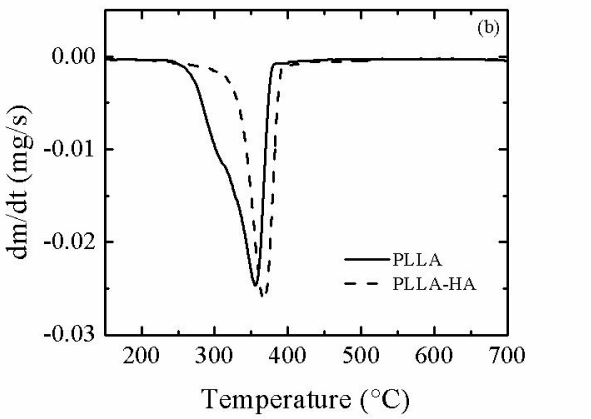

Figure 8. *Non-Isothermal (a) TGA curve and (b) DTG curve of the neat PLLA, HA and composite*

Table 3. Thermal decomposition temperatures for the PLLA composite with HA

Composite	Nanoparticle content (%)	T_{onset} (°C)	T_{peak} (°C)	E_a (KJ/mol)
PLLA-HA	0	302	355	194
	30	333	367	276

Dynamic mechanical thermal analysis of PLLA-HA composite

The influence of HA in PLLA on their mechanical behavior with temperature was evaluated by dynamic mechanical thermal analysis. Figure 9 shows the storage modulus (E') as a function of temperature for PLLA and for the composite. It can be observed that the storage modulus (E') remains slightly constant up to a specific temperature where the glass-rubber transition occurs, and then it abruptly decreases until its stabilization. This is due to the semicrystalline phase of PLLA that keeps the modulus constant. This temperature is better evaluated through the loss factor curve (Figure 10).

The addition of 30% HA to PLLA confers some reinforcement effect to the matrix at temperatures approaching the glass transition (T_g). Above this transition, the stiffness effect of HA particles maintain the structural mechanical stability of the composite at higher temperatures. Also, a possible interface interaction between the polymer matrix and HA, due to the high interfacial effect of the HA nanorods could lead to a more effective load transfer between them and therefore an improvement on the storage module was obtained. Similar results were reported in PLLA-HA composites with low nanofiller content (Wilberforce *et al.* 2011).

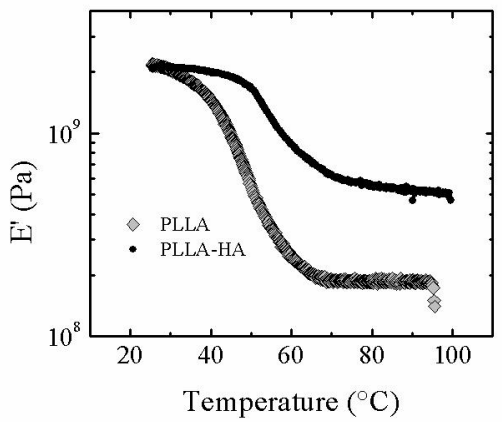

Figure 9. *DMTA Storage modulus (E') curves of the neat PLLA and the composite with HA*

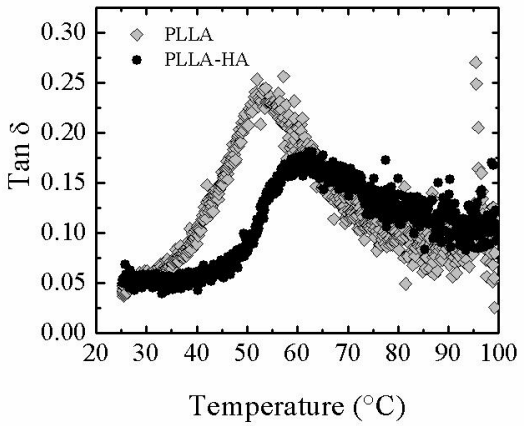

Figure 10. *DMTA Loss Factor (Tan δ) curves of the PLLA and the composite with HA*

On the other hand, the addition of HA to PLLA increased the glass transition temperature (Figure 10). The loss factor curves for PLLA and PLLA-HA composite confirm the results obtained by DSC. The peak of the curve corresponds to the glass transition relaxation. The increase in temperature associated to this relaxation is mostly due to the restriction of the cooperative motions of chain segments imposed by the presence of the rigid HA nanoparticle. As a

consequence, a better mechanical stability of the composite with temperature is obtained.

CONCLUSIONS

A composite based on PLLA-HA was prepared by the solvent casting technique and characterized in terms of its chemical, thermal and thermo-mechanical properties. The activation energy of the composite was obtained from the thermal degradation study. An interaction between the polymer matrix and HA through the carbonyl and phosphate groups was obtained by FTIR The several thermal transitions of PLLA were evaluated by DSC: the glass transition, crystallization, cold crystallization, melt-recrystallization and melting. The addition of HA to PLLA matrix increases its glass transition temperature, this was confirmed by DSC and DMTA analysis. Also, the presence of HA increases the crystallization temperature of PLLA, implying a nucleation effect. On the other hand, the cold crystallization phenomenon was suppressed by HA presence and no major changes on the melting temperature and crystallinity were observed. The PLLA-HA composite showed better thermal stability than the neat polymer. The introduction of nano-HA particles increased the decomposition temperature and the activation energy retarding the decomposition process of PLLA. The rod shape morphology of nano-HA implies a possible interfacial interaction that increases the thermal stability of the composite. Additionally, an improvement of the mechanical stability of the composite with temperature is obtained.

ACKNOWLEDGEMENTS

The authors are grateful to Prof. Alejandro Müller from the Polymer Group at Simón Bolivar University for providing the facilities for the dynamic – mechanical – thermal analysis of the samples.

REFERENCES

Aboudzadeh, N., Imani, M., Shokrgozar, M. A., Khavandi, A., Javadpour, J., Shafieyan, Y., Farokhi, M. (2010). Fabrication and characterization of poly(D,L-lactide-coglycolide)/hydroxyapatite nanocomposite scaffolds for bone tissue regeneration. J Biomed Mater Res, Part A 94A; pp. 137-145.

Albano, C., Cataño, L., Figuera, L., Perera, R., Karam, A., González, G., Noris, K. (2009). Evaluation of a composite based on high-density polyethylene filled with surface-treated hydroxyapatite. Polym Bull 62(1); pp. 45-55.

Albano, C., Cataño, L., Perera, R., Karam, A., González, G. (2010). Thermodegradative and morphological behavior of composites of HDPE with surface-treated hydroxyapatite. Polym Bull 64(1); pp. 67-79.

Albano, C., Karam, A., Perera, R., González, G., Domínguez, N., González, J., Sánchez, Y. (2006). HDPE/HA Composites obtained in solution: Effect of the gamma radiation. Nucl Instrum Methods Phys Res, Sect B 247; pp. 331-341.

Albano, C., Perera, R., Cataño, L., Alvarez, S., Karam, A., González, G. (2010). Compatibilization of polyolefin/hydroxyapatite composites using grafted polymers. Polym - Plast Technol 49(4); pp. 341-346.

Bordes, P., Pollet, E., Avérous, L. (2009). Nano-biocomposites: Biodegradable polyester/nanoclay systems. Prog Polym Sci 34; pp. 125–155.

Bourbigot, S., Flambard, X., Duquesne, S. (2001). Thermal degradation of poly(p-phenylenebenzobisoxazole) and poly(p-phenylenediamine terephthalamide) fibres. Polym Int 50; pp. 157-164.

Budrugeac, P. & Segal, E. (2001). Some methodological problems concerning nonisothermal kinetic analysis of heterogeneous solid–gas reactions. Int J Chem Kinet 33; pp. 564–573.

Coats, A. W. & Redfern, J. P. (1964). Kinetic parameters from thermogravimetric data. Nature 201; pp. 68-69.

Cui, Y., Liu, Y., Cui, Y., Jing, X., Zhang, P., Chen, X. (2009). The nanocomposite scaffold of poly(lactide-co-glycolide) and hydroxyapatite surface-grafted with L-lactic acid oligomer for bone repair. Acta Biomaterialia 5; pp. 2680-2692.

Chen, H.-J., Lai, K.-M., Lin, Y.-C. (2004). Methods for determining the kinetic parameters from nonisothermal thermogravimetry: A comparison of reliability. J Chem Eng Jpn 37(9); pp. 1172-1178.

Chłopek, J., Morawska-Chochoł, A., Paluszkiewicz, C., Jaworska, J., Kasperczyk, J., Dobrzynski, P. (2009). FTIR and NMR study of poly(lactide-co-glycolide) and hydroxyapatite implant degradation under in vivo conditions. Polym Degrad Stab 94; pp. 1479-1485.

Deplaine, H., Ribelles, J. L. G., Ferrer, G. G. (2010). Effect of the content of hydroxyapatite nanoparticles

on the properties and bioactivity of poly(L-lactide) – Hybrid membranes. Composites Science & Technology 70; pp. 1805-1812.

Grady, B. P., Paul, A., Peters, J. E., Ford, W. T. (2009). Glass Transition Behavior of Single-Walled Carbon Nanotube-Polystyrene Composites. Macromolecules 42; pp. 6152-6158.

Ivanova, T., Frank-Kamenetskaya, O., Kol'tsov, A., Ugolkov, V. (2001). Crystal structure of calcium-deficient carbonated hydroxyapatite. Thermal decomposition. J Solid State Chem 160(2); pp. 340-349.

Kim, S.-S., Park, M. S., Jeon, O., Choi, C. Y., Kim, B.-S. (2006). Poly(lactide-co-glycolide)/hydroxyapatite composite scaffolds for bone tissue engineering. Biomaterials 27; pp. 1399-1409.

Kokubo, T., Kim, H.-M., Kawashita, M. (2003). Novel bioactive materials with different mechanical properties. Biomaterials 24; pp. 2161-2175.

Kothapalli, C. R., Shaw, M. T., Wei, M. (2005). Biodegradable HA-PLA 3-D porous scaffolds: Effect of nano-sized filler content on scaffold properties. Acta Biomaterialia 1; pp. 653-662.

Kumta, P. N., Sfeir, C., Lee, D.-H., Olton, D., Choi, D. (2005). Nanostructured calcium phosphates for biomedical applications: novel synthesis and characterization. Acta Biomaterialia 1; pp. 65-83.

Lee, J. B., Lee, S. H., Yu, S. M., Park, J.-C., Choi, J. B., Kim, J. K. (2008). PLGA scaffold incorporated with hydroxyapatite for cartilage regeneration. Surface & Coatings Technology 202; pp. 5757-5761.

Li, J., Chen, Y., Maka, A. F. T., Tuan, R. S., Li, L., Li, Y. (2010). A one-step method to fabricate PLLA scaffolds with deposition of bioactive hydroxyapatite and collagen using ice-based microporogens. Acta Biomaterialia 6; pp. 2013-2019.

Li, L. H., Kommareddy, K. P., Pilz, C., Zhou, C. R., Fratzl, P., Manjubala, I. (2010). In vitro bioactivity of bioresorbable porous polymeric scaffolds incorporating hydroxyapatite microspheres. Acta Biomaterialia 6; pp. 2525-2531.

Li, Z. & Wang, P. (2005). Preparation of nanosized hydroxyapatite particles at low temperatures. J Mater Sci 40; pp. 6589-6591.

Mamleev, V., Bourbigot, S., Bras, M. L., Duquesne, S., Sestak, J. (2000). Modelling of nonisothermal kinetics in thermogravimetry. Phys Chem Chem Phys 2; pp. 4708-4716.

Mcneill, I. C. & Leiper, H. A. (1985). Degradation studies of some polyesters and polycarbonates—2. Polylactide: Degradation under isothermal conditions, thermal degradation mechanism and photolysis of the polymer. Polym Degrad Stab 11; pp. 309-326.

Nair, L. S., Laurencin, C. T. (2007). Biodegradable polymers as biomaterials. Prog Polym Sci 32; pp. 762-798.

Nejati, E., Mirzadeh, H., Zandi, M. (2008). Synthesis and characterization of nano-hydroxyapatite rods/poly(L-lactide acid) composite scaffolds for bone tissue engineering. Composites: Part A 39; pp. 1589-1596.

Pavlidoua, S. & Papaspyridesb, C. D. (2008). A review on polymer–layered silicate nanocomposites. Prog Polym Sci 33; pp. 1119–1198.

Peng, F., Yu, X., Wei, M. (2011). In vitro cell performance on hydroxyapatite particles/poly(L-lactic acid) nanofibrous scaffolds with an excellent particle along nanofiber orientation. Acta Biomaterialia 7; pp. 2585-2592.

Petricca, S. E., Marra, K. G., Kumta, P. N. (2006). Chemical synthesis of poly(lactic-co-glycolic acid)/hydroxyapatite composites for orthopaedic applications. Acta Biomaterialia 2; pp. 277-286.

Pham, J. Q., Mitchell, C. A., Bahr, J. L., Tour, J. M., Krishanamoorti, R., Green, P. F. (2003). Glass Transition of Polymer/Single-Walled Carbon Nanotube Composite Films. J Polym Sci, Part B: Polym Phys 41; pp. 3339-3345.

Reyes-De-Vaaben, S., Aguilar, A., Avalos, F., Ramos-De-Valle, L. F. (2008). Carbon nanoparticles as effective nucleating agents for polypropylene. J Therm Anal Calorim 93; pp. 947-952.

Rezwan, K., Chen, Q. Z., Blaker, J. J., Boccaccini, A. R. (2006). Biodegradable and bioactive porous polymer/inorganic composite scaffolds for bone tissue engineering. Biomaterials 27; pp. 3413-3431.

Roeder, R. K., Converse, G. L., Kane, R. J., Yue, W. (2008). Hydroxyapatite-Reinforced Polymer Biocomposites for Synthetic Bone Substitutes. JOM 60; pp. 38-45.

Sahoo, N. G., Rana, S., Chob, J. W., Li, L., Chan, S. H. (2010). Polymer nanocomposites based on functionalized carbon nanotubes. Prog Polym Sci 35; pp. 837-867.

Seyedjafari, E., Soleimani, M., Ghaemi, N., Shaban, I. (2010). Nanohydroxyapatite-Coated Electrospun Poly(L-lactide) Nanofibers Enhance Osteogenic Differentiation of Stem Cells and Induce Ectopic Bone Formation. Biomacromolecules 11; pp. 3118-3125.

Shikinami, Y. & Okuno, M. (1999). Bioresorbable devices made of forged composites of hydroxyapatite (HA) particles and poly-L-lactide (PLLA): Part I. Basic characteristics. Biomaterials 20; pp. 859-877.

Spadavecchia, U. & González, G. (2007). Nanometric hydroxyapatite synthesis for medical applications Rev Fac Ing UCV 22(4); pp. 37-44.

Spitalsky, Z., Tasis, D., Papagelis, K., Galiotis, C. (2010). Carbon nanotube–polymer composites: Chemistry, processing, mechanical and electrical properties. Prog Polym Sci 35; pp. 357-401.

Velde, K. V. D. & Kiekens, P. (2002). Biopolymers: overview of several properties and consequences on their applications. Polym Test 21; pp. 433-442.

Wang, A., Yin, H., Liu, D., Wu, H., Wada, Y., Ren, M., Xu, Y., Jiang, T., Cheng, X. (2007). Effects of organic modifiers on the size-controlled synthesis of hydroxyapatite nanorods Appl Surf Sci 6; pp. 3311-3316.

Wang, Y. & Mano, J. F. (2005). Role of thermal history on the thermal behavior of Poly(l-lactic acid) studied by dsc and optical microscopy. J Therm Anal Calorim 80; pp. 171-175.

Wilberforce, S. I. J., Finlayson, C. E., Best, S. M., Cameron, R. E. (2011). The influence of hydroxyapatite (HA) microparticles (m) and nanoparticles (n) on the thermal and dynamic mechanical properties of poly-L-lactide. Polymer 52; pp. 2883-2890.

Yasuniwa, M., Tsubakihara, S., Sugimoto, Y., Nakafuku, C. (2004). Thermal Analysis of the Double-Melting Behavior of Poly(L-lactic acid). J Polym Sci, Part B: Polym Phys 42; pp. 25-32.

Zhang, C. Y., Lu, H., Zhuang, Z., Wang, X. P., Fang, Q. F. (2010). Nano-hydroxyapatite/poly(L-lactic acid) composite synthesized by a modified in situ precipitation: preparation and properties. J Mater Sci: Mater Med 21; pp. 3077-3083.

Zhou, S., Zheng, X., Yu, X., Wang, J., Weng, J., Li, X., Feng, B., Yin, M. (2007). Hydrogen Bonding Interaction of Poly(D,L-Lactide)/hydroxyapatite Nanocomposites. Chem Mater 19; pp. 247-253.